



# The Relation between the Perturbative QCD Scale $\Lambda_s$ and Hadronic Masses from Light-Front Holography

A. Deur<sup>a,1</sup>, S. J. Brodsky<sup>b</sup>, G. F. de Teramond<sup>c</sup><sup>a</sup>Thomas Jefferson National Accelerator Facility, Newport News, VA 23606, USA<sup>b</sup>SLAC National Accelerator Laboratory, Stanford University, Stanford, California 94309, USA<sup>c</sup>Universidad de Costa Rica, San José, Costa Rica

## Abstract

QCD is well understood at short distances where perturbative calculations are feasible. Establishing an explicit analytic connection between the short-distance regime and the large-distance physics of quark confinement has been a long-sought goal. A major challenge is to relate the scale  $\Lambda_s$  underlying the evolution of the QCD coupling in the perturbative regime to the masses of hadrons. We show here how new theoretical insights into the behavior of QCD at large distances leads to such a relation. The resulting prediction for  $\Lambda_s$  in the  $\overline{MS}$  scheme agrees well with experimental measurements. Conversely, the relation can be used to predict the masses of hadrons composed of light quarks with the measured value of  $\Lambda_s$  as the sole parameter. We also use “light-front holography” to determine the analytic form of  $\alpha_s(Q^2)$  at small  $Q^2$ .

**Keywords:** QCD,  $\Lambda_s$ , Strong coupling  $\alpha_s$ , Hadron spectrum, AdS/CFT, Light Front holography.

## 1. Introduction

The masses of hadrons composed of light quarks such as the proton and  $\rho$  meson are understood to originate from the energy of the confining interactions of QCD; however, it is unclear why the typical hadron mass scale is of order 1 GeV. One would expect this mass scale to be explicitly present in the QCD Lagrangian. However, the only scale in  $\mathcal{L}_{QCD}$  are the quark masses, which for the up and down quarks, are evidently too small to be relevant:  $m_q \sim 10^{-3}$  GeV. A relevant mass scale,  $\Lambda_s$ , however, does exist. It controls the strength of the coupling of quarks when they interact at short distances. Its precise definition emerges when one renormalizes the QCD coupling  $\alpha_s(Q^2)$ . The results presented in this

talk can be discussed in any choice of renormalization scheme, but we will use here the value of  $\Lambda_s$  defined in the  $\overline{MS}$  (modified minimal subtraction) renormalization scheme. The value of the parameter  $\Lambda_s = \Lambda_{\overline{MS}}$  can be determined to high precision from experimental measurements of high-energy, short-distance processes where the strength of QCD is small because of asymptotic freedom [1, 2] and perturbative QCD (pQCD) is thus applicable. One long-sought goal in QCD is to find an explicit relation between the hadron masses and  $\Lambda_s$ .

In this talk we present such relation [3], which leads to the prediction of the value of  $\Lambda_s$  from a hadronic mass. Conversely, one can obtain the hadronic spectrum using  $\Lambda_s$ . To establish this relation, we use the QCD effective coupling  $\alpha_s$  computed at small-distance using pQCD and at long distance using the formalism of QCD on the Light Front which allows, under reasonable approximations, non-perturbative calculations. We will also use “light-front holography” to determine the precise form of  $\alpha_s(Q^2)$  at small  $Q^2$ . The small and large distance regimes of QCD overlap, a phenomenon

\*Talk given at 18th International Conference on Quantum Chromodynamics (QCD 15, 30th anniversary), 29 June - 3 July 2015, Montpellier, France

\*\*Preprint: JLAB-PHY-15-2135; SLAC-PUB-16385

Email address: deurpam@jlab.org (A. Deur)

<sup>1</sup>Speaker, Corresponding author.

related to “quark-hadron duality” [4]. This allows us to match the two descriptions and obtain the behavior of  $\alpha_s(Q^2)$  at any scale. This in turn leads to an analytical relation between  $\Lambda_s$  and hadron masses.

## 2. Light-Front QCD

The light-front (LF) quantization procedure is based on the “Front Form” invented by Dirac [5], where the time evolution variable is  $\tau = t + z/c$ ; *i.e.*, time along the light-front. The resulting LF Hamiltonian and its eigensolutions are Lorentz frame-independent [6].

One can derive a one-dimensional “light-front Schrödinger equation” (LFSE) in QCD describing the valence Fock state of color-singlet  $q\bar{q}$  mesons for light quarks, analogous to the Schrödinger equation describing hydrogenic atoms in QED [7]. Unlike the QED form, the LFSE is relativistic and frame-independent. The radial variable for the LFSE, the invariant separation between the  $q$  and  $\bar{q}$  is  $\zeta = b_\perp \sqrt{x(1-x)}$ , where  $\zeta^2$  is conjugate to the LF kinetic energy  $k_\perp^2/(x(1-x))$ , the invariant mass squared of the  $q\bar{q}$ . Here  $b_\perp$  is the transverse impact parameter and  $x$  is the LF momentum fraction  $x = k^+/P^+ = (k^0 + k^z)/(P^0 + P^z)$ . The LFSE incorporates color confinement and other essential spectroscopic and dynamical features of hadron physics, including a massless pion for zero quark mass and linear Regge trajectories with the same slope in the radial quantum number  $n$  and internal orbital angular momentum  $L$ .

The form of the LF potential  $V(\zeta^2)$  entering the LFSE -its sole unspecified component- becomes uniquely determined as a harmonic oscillator  $V(\zeta^2) = \kappa^4 \zeta^2$  when one extends the formalism of de Alfaro, Fubini and Furlan (dAFF) [8] to light-front Hamiltonian theory [9]. This discovery by dAFF, in the context of  $1 + 1$  quantum mechanics, allows for the emergence in the theory of a mass scale  $\kappa$  without it appearing explicitly in the Lagrangian. That is, enforcing the conformal symmetry of QCD fully determines the confinement potential  $\kappa^4 \zeta^2$  in the LFSE underlying the hadron spectrum.

The harmonic oscillator form of the LF potential corresponds to a linear potential for bound states of heavy quarks in the usually employed instant-form [10]. This links a semi-classical approximation to light-front QCD, based on the underlying conformality of QCD in the limit of zero quark masses, to lattice gauge theory and other approaches to heavy quark effective theory. The parameter  $\kappa$  is obtained from a hadron mass, *e.g.*  $\kappa = M_\rho/\sqrt{2}$  [11]. This provides a rather model-independent tractable formalism for addressing the non-perturbative QCD bound-state problem at leading order.

## 3. LF holography

We have stressed the importance of the conformal symmetry for QCD. The conformal group in four dimensions is geometrically represented by the five-dimensional AdS<sub>5</sub> space. It is holographically dual to 3+1 spacetime using light-front time  $\tau$ . In this correspondence the LF variable  $\zeta$  can be identified with the fifth AdS dimension. For hadrons probed at short distances  $\zeta \sim 1/Q^2$ , with  $Q^2$  the 4-momentum squared exchanged between the hadron and a beam particle.

Remarkably, the same confining LF potential  $V(\zeta^2) = \kappa^4 \zeta^2$  and the same LFSE for mesons of arbitrary spin  $J$  can be derived [12] from the “soft-wall model” [13] modification of AdS<sub>5</sub> space assuming the specific “dilaton profile”  $e^{+\kappa^2 z^2}$ . Using LF Holography, one can identify the fifth dimension coordinate  $z$  of AdS<sub>5</sub> space with the light-front coordinate  $\zeta$ . This correspondence, often called AdS/QCD, is well established: there exists a one-to-one mapping between LF and AdS wavefunctions. Furthermore, the expressions for the electromagnetic and gravitational form factors of hadrons in AdS<sub>5</sub> are the same as the Drell-Yan West formula in 3+1 space using LF time [14]. All in all, the AdS/QCD correspondence provides an excellent description of hadrons of arbitrary spin, incorporating many of observed spectroscopic and dynamical features [7, 9, 11, 12, 14].

## 4. Determining $\alpha_s$ at all scales

### 4.1. $\alpha_s$ at small $Q^2$ from LF Holography

One can derive the explicit form for  $\alpha_s(Q^2)$  from LF-QCD using AdS/QCD. As noted above, the forces that bind quarks are related in AdS/QCD to the modification of the AdS space curvature, the dilaton profile  $e^{+\kappa^2 z^2}$  encoding confinement dynamics [9]. This modification of the AdS geometry is constrained by the form of the potential dictated by the dAFF mechanism. The same constraint also prescribes the form of  $\alpha_s$  at small  $Q^2$ .

In pQCD, the effective coupling  $\alpha_s(Q^2)$  is defined at high  $Q^2$  by folding short-distance quantum effects into its evolution. Analogously, as we will show, the  $Q^2$ -dependence of the AdS/QCD effective coupling stems from the effects of the large-distance forces folded into the coupling constant [15].

To determine  $\alpha_{g_1}^{AdS}$ , consider first the AdS action. It has the same form as General Relativity’s action:

$$S \propto \int d^4x \sqrt{\det(g_{\mu\nu})} \frac{R}{G_N}, \quad (1)$$

but with  $R$ , the Ricci scalar, and  $G_N$ , Newton’s constant, replaced by their QCD-analogs. Thus  $\sqrt{R}$  is

replaced by the gluon field  $F$ ,  $\sqrt{G_N}$  corresponds to the gauge coupling  $g_{AdS}$ , and the metric determinant is  $\sqrt{\det(g_{\mu\nu}^{AdS})} e^{\kappa^2 z^2}$ , which includes the  $e^{\kappa^2 z^2}$  dilaton profile. The 5-dimensional AdS action is thus:

$$S = \frac{1}{4} \int d^5x \sqrt{\det(g_{\mu\nu}^{AdS})} e^{\kappa^2 z^2} \frac{1}{g_{AdS}^2} F^2. \quad (2)$$

In pQCD,  $\alpha_s \equiv g_s^2/4\pi$  acquires its  $Q^2$ -dependence from short-distance quantum effects. Similarly, the initially constant AdS coupling  $\alpha_{AdS} \equiv g_{AdS}^2/4\pi$  is re-defined to absorb the effects of the AdS deformation:  $g_{AdS}^2 \rightarrow g_{AdS}^2 e^{\kappa^2 z^2}$ . Transforming to momentum space yields [15]

$$\alpha_{g_1}^{AdS}(Q^2) = \pi \exp\left(\frac{-Q^2}{4\kappa^2}\right). \quad (3)$$

Here,  $\alpha_{g_1}^{AdS}(Q^2)$ , the effective charge in the  $g_1$ -scheme defined from the Bjorken sum rule [16, 17], is normalized to  $\pi$  at  $Q^2 = 0$  due to fulfill straightforward kinematical constraints [18, 19]. This coupling can serve as the QCD-analog of the Gell-Mann-Low coupling  $\alpha(Q^2)$  of QED [15]. Since LF-holography neglects quantum effects, the short-distance phenomena which lead to the pQCD evolution of the running of pQCD coupling are not incorporated in  $\alpha_{AdS}$ . Indeed, the Gaussian form of Eq. (3) falls much faster than the pQCD prediction at large  $Q^2$ .

#### 4.2. Behavior of $\alpha_s$ at large $Q^2$

The large  $Q^2$ -dependence of  $\alpha_s(Q^2)$  is well known [20]. Its evolution is given by the QCD renormalization group equation where the logarithmic derivative of the coupling defines the  $\beta$  function. If  $\alpha_s$  is small, one can use the perturbative expansion:

$$Q^2 d\alpha_s/dQ^2 = -(\beta_0\alpha_s^2 + \beta_1\alpha_s^3 + \beta_2\alpha_s^4 + \dots). \quad (4)$$

The  $\beta_i$  for  $i \geq 2$  are scheme-dependent and are known up to order  $\beta_3$  in the  $\overline{MS}$  renormalization scheme [20]. Eq. (4) thus yields  $\alpha_{\overline{MS}}(Q^2)$  at high  $Q^2$ . In addition,  $\alpha_{g_1}^{pQCD}(Q^2)$  can be expressed as a perturbative expansion in  $\alpha_{\overline{MS}}(Q^2)$  [16, 17]. Thus, pQCD predicts the form of  $\alpha_{g_1}(Q^2)$  at large  $Q^2$ :

$$\alpha_{g_1}^{pQCD}(Q^2) = \pi \left[ \alpha_{\overline{MS}}/\pi + a_1 (\alpha_{\overline{MS}}/\pi)^2 + a_2 (\alpha_{\overline{MS}}/\pi)^3 + a_3 (\alpha_{\overline{MS}}/\pi)^4 + \dots \right]. \quad (5)$$

The coefficients  $a_i$  are known up to order  $a_3$  [21].

Eqs. (3) and (5) thus provide  $\alpha_{g_1}(Q^2)$  in the large and small distance regimes, respectively.

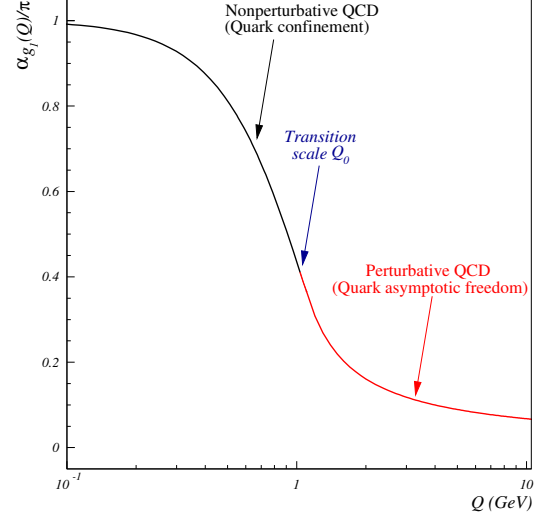


Figure 1: The strong coupling obtained from the analytic matching of perturbative and non-perturbative QCD regimes.

### 5. Relation between $\Lambda_{\overline{MS}}$ and hadron masses

The existence at moderate values of  $Q^2$  of a dual description of QCD in terms of either quarks and gluons versus hadrons (“quark-hadron duality” [4]) is consistent with the matching of  $\alpha_{g_1}^{pQCD}$  to  $\alpha_{g_1}^{AdS}$  at intermediate values of  $Q^2$ . This matching can be done by imposing continuity of both  $\alpha_{g_1}(Q^2)$  and their derivatives, as shown in Fig. 1. The unique solution for the resulting two equalities determines  $\Lambda_s$  from  $\kappa$ , and fixes the scale  $Q_0$  characterizing the transition between the large and short-distance regimes of QCD. At leading-order, the system can be solved analytically. It yields:

$$\Lambda_{\overline{MS}} = M_\rho e^{-(a+1)}/\sqrt{a}, \quad (6)$$

with  $a = 4(\sqrt{\ln(2)^2 + 1 + \beta_0/4} - \ln(2))/\beta_0$ . For  $n_f = 3$  quark flavors,  $a \simeq 0.55$ . The system was solved numerically at higher orders. The result at order  $\beta_3$ , the same order to which the experimental value of  $\Lambda_{\overline{MS}}$  is extracted, is  $\Lambda_{\overline{MS}} = 0.341 \pm 0.024$  GeV for  $n_f = 3$ . The uncertainty stems from the extraction of  $\kappa$  from the  $\rho$  or proton masses and from a small contribution from ignoring the quark masses.

This theory uncertainty is less or comparable to that of the measurements, which combine to  $\Lambda_{\overline{MS}} = 0.339 \pm 0.016$  GeV [20]. In Fig. 2 we compare our calculation with the best measurements, recent lattice results and their average,  $\Lambda_{\overline{MS}} = 0.340 \pm 0.008$  GeV [20]. In Fig. 3, the AdS/QCD prediction of  $\alpha_{g_1}^{AdS}(Q^2)$  (3) is plotted together with data [18, 19]. Even though it has no adjustable parameters, the predicted Gaussian form for the

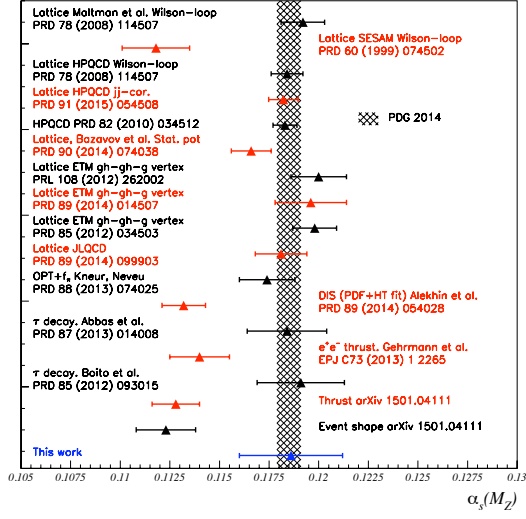


Figure 2: Comparison between our result and determinations of  $\alpha_{\overline{MS}}(M_Z)$  from the high precision experimental and lattice measurements. The world average [20] is shown as the vertical band.

behavior of  $\alpha_{g_1}^{AdS}(Q^2)$  at  $Q^2 \lesssim 1 \text{ GeV}^2$  agrees well with data [15]. Also shown in this figure is the very small dependence of  $\alpha_{g_1}^{pQCD}(Q^2)$  on the  $\beta_n$  and  $\alpha_{\overline{MS}}^5$  orders used in Eqs. (4) and (5), respectively.

The matching of the soft and hard domains of the running coupling  $\alpha_{g_1}(Q^2)$  also determines the transition scale  $Q_0$ . At order  $\beta_3$ ,  $Q_0^2 \approx 1.25 \pm 0.19 \text{ GeV}^2$ . This value is similar to the traditional lower limit  $Q^2 > 1 \text{ GeV}^2$  used for pQCD. An approximate value similar to ours was found in Ref. [22], which terminates the evolution of  $\alpha_s(Q^2)$  near  $Q \approx 1 \text{ GeV}$  in order to enforce quark-hadron duality for the proton structure function  $F_2(x, Q^2)$  measured in deep-inelastic experiments.

## 6. Determination of the hadron spectrum

Instead of predicting  $\Lambda_{\overline{MS}}$  from  $\kappa$ , one can, conversely, predict the hadron mass spectrum using the world average  $\Lambda_{\overline{MS}} = 0.340 \pm 0.008 \text{ GeV}$  [20] as the only input. One obtains  $M_\rho = 0.777 \pm 0.051 \text{ GeV}$ , in near perfect agreement with the measured  $M_\rho = 0.775 \pm 0.000 \text{ GeV}$  [20]. The theory uncertainty stems from the truncation of the series, Eq. (5), from the uncertainty on  $\Lambda_{\overline{MS}}$  [20], and from the truncation of the  $\beta$  series, Eq. (4). The computed proton and neutron masses, however, are  $2\sigma$  higher than the averaged experimental values,  $M_N = 1.092 \pm 0.073 \text{ GeV}$  compared to  $0.939 \pm 0.000 \text{ GeV}$ . Other meson and baryon masses are calculated as orbital and radial excitations of the LF-QCD Schroedinger equation [11, 12]. The

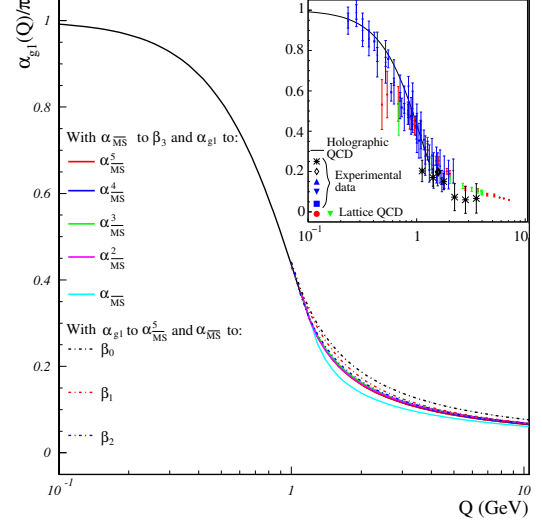


Figure 3: The dependence of  $\alpha_{g_1}$  on the orders of the  $\beta$  and  $\alpha_{\overline{MS}}^5$  series. The continuous black line is  $\alpha_{g_1}^{AdS}$ . The continuous colored lines are the matched  $\alpha_{g_1}^{pQCD}$  for all available orders in the  $\alpha_{\overline{MS}}^5$  series (the order of the  $\beta$  series was kept at  $\beta_3$ ). The dash-dotted colored lines are the matched  $\alpha_{g_1}^{pQCD}$  at different orders in the  $\beta$  series (the order of the series was kept at  $\alpha_{\overline{MS}}^5$ ). The comparison between  $\alpha_{g_1}^{AdS}$  and the data is shown in the embedded figure. This comparison is shown within the range of validity of AdS/QCD.

predictions are shown in Figs. 4 and 5 for the vector mesons. Thus, using  $\Lambda_{\overline{MS}}$  as the only input, the hadron mass spectrum is calculated self-consistently within the holographic QCD framework.

## 7. Summary

We have presented an explicit relation between the quark-confining nonperturbative dynamics of QCD at large-distances and the short-distance dynamics of pQCD; we thus can link the pQCD scale  $\Lambda_s$  to the observed hadron masses. The predicted value  $\Lambda_{\overline{MS}} = 0.341 \pm 0.024 \text{ GeV}$  agrees well with the experimental average  $0.339 \pm 0.016 \text{ GeV}$  and the lattice average  $0.340 \pm 0.008 \text{ GeV}$ . Conversely, we can predict the value of  $\kappa$  and the hadron mass spectrum for light quarks using the experimental value of  $\Lambda_s$  as the sole input parameter.

We have used an effective theory which encodes the underlying conformality of QCD and the emergence of a scale through the dAFF procedure. Together with light-front holography, the duality between  $AdS_5$  space and physical  $3+1$  space at fixed LF time  $\tau$  allow us to determine both the color confining potential in the Light-Front Schrödinger Equation  $U(\zeta^2) = \kappa^4 \zeta^2$  and the analytic form of the running coupling  $\alpha_s(Q^2)/\pi =$

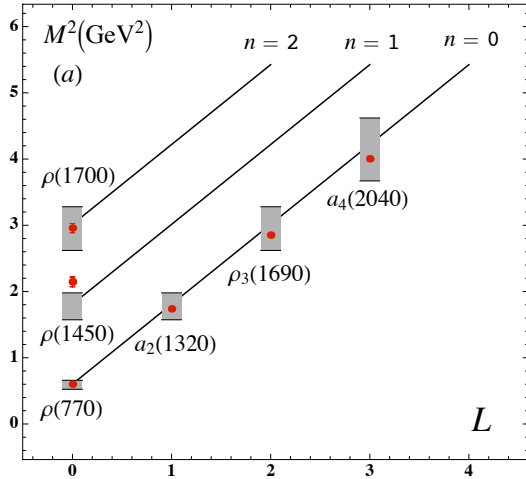


Figure 4: The predicted mass spectrum for the light vector mesons as a function of the internal orbital angular momentum  $L$  and the radial excitation  $n$  for unflavored mesons. The red dots are the experimental values. The dark lines represent the results discussed here and the gray bands the uncertainty. The only parameter entering this determination is the world average  $\Lambda_{\overline{MS}} = 0.340 \pm 0.008$  GeV. The decay widths of the mesons are not accounted for in the calculation.

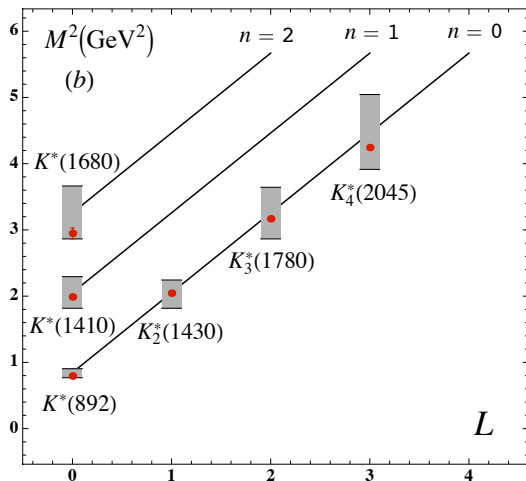


Figure 5: Same as Fig. 4 but for strange mesons. Only two parameters, the strange quark mass and  $\Lambda_{\overline{MS}}$  are used to obtain this spectrum.

$\exp(-Q^2/4\kappa^2)$  at small  $Q^2$ . The predicted Gaussian form agrees remarkably with the running of the effective charge determined from measurements of the  $Q^2$  dependence of the Bjorken sum rule, in effect, without any free parameters.

It should be emphasized that QCD has no knowledge of conventional units of mass such as GeV; thus only ratios can be predicted from QCD alone. The value of  $\kappa$  in GeV never needs to be determined. Consequently our work predicts ratios such as  $\Lambda_s/\kappa$  and  $\Lambda_s/M_H$  where  $M_H$  is any hadron mass. For the same reason, only the ratio  $\Lambda_{\overline{MS}}/F_\pi$  is evaluated in Ref. [23].

**Acknowledgments.** This material is based upon work supported by the U.S. Department of Energy, Office of Science, Office of Nuclear Physics under contract DE-AC05-06OR23177. This work is also supported by the Department of Energy contract DE-AC02-76SF00515.

## References

- [1] D. J. Gross and F. Wilczek, Phys. Rev. Lett. **30**, 1343 (1973).
- [2] H. D. Politzer, Phys. Rev. Lett. **30**, 1346 (1973).
- [3] A. Deur, S. J. Brodsky and G. F. de Teramond, arXiv:1409.5488 [hep-ph].
- [4] E. D. Bloom and F. J. Gilman, Phys. Rev. Lett. **25** 1140 (1970).
- [5] P. A. M. Dirac, Rev. Mod. Phys. **21**, 392 (1949).
- [6] S. J. Brodsky, H. C. Pauli and S. S. Pinsky, Phys. Rep. **301**, 299 (1998).
- [7] G. F. de Teramond and S. J. Brodsky, Phys. Rev. Lett. **102**, 081601 (2009).
- [8] V. de Alfaro, S. Fubini and G. Furlan, Nuovo Cim. A **34**, 569 (1976).
- [9] S. J. Brodsky, G. F. de Teramond and H. G. Dosch, Phys. Lett. B **729**, 3 (2014).
- [10] A. P. Trawinski *et al.*, Phys. Rev. D **90** (2014) 074017.
- [11] For a review see: S. J. Brodsky, G. F. de Teramond, H. G. Dosch and J. Erlich, Phys. Rept. **584**, 1 (2015).
- [12] G. F. de Teramond, H. G. Dosch and S. J. Brodsky, Phys. Rev. D **87**, 075005 (2013).
- [13] A. Karch, E. Katz, D. T. Son and M. A. Stephanov, Phys. Rev. D **74**, 015005 (2006).
- [14] S. J. Brodsky and G. F. de Teramond, Phys. Rev. Lett. **96**, 201601 (2006).
- [15] S. J. Brodsky, G. F. de Teramond and A. Deur, Phys. Rev. D **81**, 096010 (2010).
- [16] J. D. Bjorken, Phys. Rev. **148**, 1467 (1966).
- [17] J. D. Bjorken, Phys. Rev. D **1**, 1376 (1970).
- [18] A. Deur, V. Burkert, J. P. Chen and W. Korsch, Phys. Lett. B **650**, 244 (2007).
- [19] A. Deur, V. Burkert, J. P. Chen and W. Korsch, Phys. Lett. B **665**, 349 (2008).
- [20] K. A. Olive *et al.* (Particle Data Group), Chin. Phys. C, **38**, 090001 (2014).
- [21] P. A. Baikov, K. G. Chetyrkin and J. H. Kuhn, Phys. Rev. Lett. **104**, 132004 (2010).
- [22] A. Courtoy and S. Liuti, Phys. Lett. B **726**, 320 (2013).
- [23] J.-L. Kneur and A. Neveu, Phys. Rev. D **85**, 014005 (2012); Phys. Rev. D **88**, 074025 (2013).